

Detailed investigation of the temperature dependence of ionic transport parameters of a new composite electrolyte system $(1 - x)$ $(0.75\text{AgI}:0.25\text{AgCl}):x\text{SnO}_2$

R. C. AGRAWAL* and R. K. GUPTA

Solid State Ionics Research Laboratory, School of Studies in Physics, Pt. Ravishankar Shukla University, Raipur 492 010, India

Detailed investigations of a new Ag^+ -ion-conducting two-phase composite electrolyte system $(1 - x)$ $(0.75\text{AgI}:0.25\text{AgCl}):x\text{SnO}_2$ are reported, where $0 \leq x \leq 50$ in weight per cent. A "quenched-and-annealed $(0.75\text{AgI}:0.25\text{AgCl})$ mixed system–solid solution" was used as the first phase instead of the commonly used host matrix salt AgI. Micron-sized particles (about $10 \mu\text{m}$) of SnO_2 were dispersed in the first (matrix) phase. The composition $0.8(0.75\text{AgI}:0.25\text{AgCl}):0.2\text{SnO}_2$ exhibited conductivity enhancements of more than eight times over the annealed host and about three times over the quenched host at room temperature and has been referred to as "optimum composition". The existence of two separate phases has been ascertained by X-ray diffraction and differential thermal analysis techniques. The temperature dependence of the electrical conductivity, σ , ionic mobility, μ , mobile ion concentration, n , ionic transference number, t_{ion} , and ionic drift velocity, v_d , are also reported. The enhancement in the conductivity in this two-phase composite electrolyte has been attributed to the increase in ionic mobility at room temperature.

1. Introduction

Room-temperature enhancements of approximately one to three orders of magnitude have been reported in many heterogeneously doped two-phase Ag^+ -ion-conducting composite electrolyte systems [1–7]. These systems are fabricated simply by controlled dispersion of ultrafine particles of an insulating and chemically inert material, namely, Al_2O_3 or SiO_2 or Fe_2O_3 or fly-ash (referred to as second-phase dispersoids), into the moderately ionic conducting silver halide, namely, AgI or AgBr or AgCl (referred to as the first-phase host matrix). The mechanism of conductivity enhancements in these systems can be understood on the basis of the increased mobile ion concentration at the host–dispersoid interface region and/or increased ionic mobility due to the creation of highly conducting paths interconnecting these regions [8–17]. The volume fraction of the second-phase dispersoid and its particle size are critical factors which decide optimum conductivity in these systems [1–4, 6].

The majority of the fast-silver-ion-conducting composite systems are prepared using AgI as the first-phase host matrix, in general. In a recent investigation, we suggested an alternative compound: "a

quenched-and-annealed $(0.75\text{AgI}:0.25\text{AgCl})$ mixed system", in place of the conventional host AgI [18, 19], exhibiting many transport properties superior to AgI. We have also reported that the new host yields much better composite electrolyte [20, 21] and glass systems [22–24]. In this paper, we report the preparation and transport property studies on a new Ag^+ -ion-conducting two-phase composite system: $(1 - x)$ $(0.75\text{AgI}:0.25\text{AgCl}):x\text{SnO}_2$, where $x = 0.1, 0.15, 0.2, 0.25, 0.3, 0.4$ and 0.5 in weight fraction. The chemically inert and insoluble SnO_2 was used as the second-phase dispersoid. For direct comparison of room-temperature conductivity, the composite systems $(1 - x)\text{AgI}:x\text{SnO}_2$ were also prepared in an identical manner using the conventional host AgI. Various experimental studies carried out on the new composite system are outlined below.

1. Compositional variation in room-temperature conductivity, σ , will enable us to determine the optimum conducting composition.
2. X-ray diffraction (XRD) and differential thermal analysis (DTA) studies on the optimum composition will allow us to identify the existence of two separate phases.

* Author to whom all correspondence should be addressed.

3. The temperature dependences of the electrical conductivity, ionic mobility, μ , mobile ion concentration, n , ionic transference number, t_{ion} , and ionic drift velocity, v_d , will permit us to evaluate the energies involved in different thermally activated processes and to give plausible reasons to explain the ion transport mechanism in this system.

2. Experimental procedure

Commercially available pre-dried chemicals AgI (purity, greater than 98%), AgCl (purity, greater than 99%) (Reidel (India) Chemicals) and SnO₂ (purity, greater than 99%; particle size, about 10 μ m) (CDH, India) were used, without further purification, for the preparation of the composite systems $(1-x)(0.75\text{AgI}:0.25\text{AgCl}):x\text{SnO}_2$, where $0 \leq x \leq 50$ in weight per cent or $0 \leq x \leq 0.5$ in weight fraction. Several sample preparation sequences were adopted, as also described in an earlier paper [21]. Various routes of sample preparation attempted in the present study are given below.

Route 1: homogeneous mixtures of (quenched-and-annealed $(0.75\text{AgI}:0.25\text{AgCl}) + \text{SnO}_2$) in different weight fractions, in separate silica tubes were heated above 600 °C for 15 min (i.e., soaking time) and then quenched rapidly with a cooling rate of about 10^2 K s^{-1} .

Route 2: (annealed $(0.75\text{AgI}:0.25\text{AgCl}) + \text{SnO}_2$) in different weight fractions were heated to about 600 °C for 15 min and then annealed at about 200 °C for 24 h.

Route 3: simple physical mixture of (quenched $(0.75\text{AgI}:0.25\text{AgCl}) + \text{SnO}_2$) in different weight fractions were used.

Route 4: physical mixture of (annealed $(0.75\text{AgI}:0.25\text{AgCl}) + \text{SnO}_2$) in different weight fractions were annealed at 200 °C for 24 h.

Samples of the composite system $(1-x)\text{AgI}:x\text{SnO}_2$ were also prepared by route 1 using the conventional host AgI. The finished products were finely ground and pressed (about 2 ton. cm^{-2}) to pellets 0.75–2 mm in thickness and about 1.185 cm in diameter. Colloidal silver paint was applied onto both surfaces of the pellets as electrodes for conductivity measurements. Phase identification and material characterization studies were carried out by XRD and DTA techniques. The temperature dependences of various transport properties, namely, the electrical conductivity, σ , ionic mobility, μ , mobile ion concentration, n , ionic transference number, t_{ion} , and ionic drift velocity, v_d , were studied using different techniques as discussed by us in our earlier papers [18–24].

3. Results and discussion

3.1. Electrical conductivity as a function of composition and temperature: effect of preparation route and soaking time

Fig. 1 shows the compositional variation of room-temperature conductivity for the composite system $(1-x)(0.75\text{AgI}:0.25\text{AgCl}):x\text{SnO}_2$ fabricated via routes 1–4, mentioned in Section 2, where $x = 0, 10, 15, 20, 25, 30, 40, 50$ in weight per cent. A similar plot

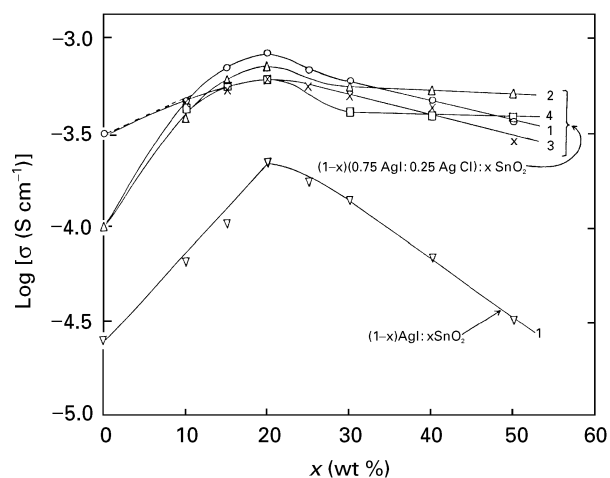


Figure 1 log σ versus x plots at about 300 K for the composite electrolyte systems $(1-x)(0.75\text{AgI}:0.25\text{AgCl}):x\text{SnO}_2$ and $(1-x)\text{AgI}:x\text{SnO}_2$. The numbers 1–4 correspond to the different preparation routes (see text).

for the system $(1-x)\text{AgI}:x\text{SnO}_2$, prepared by route 1, is also drawn in Fig. 1 for direct comparison. The σ – x variations for both the systems followed the usual behaviour of most composite electrolytes [1–6], i.e., σ increased initially with increasing x , attained a peak value and then decreased. Some of the noteworthy features of this study are as follows.

1. Conductivity enhancements have been achieved in both composite systems; however, the new host resulted in a better solid electrolyte system because it has superior transport properties to those of AgI.

2. No marked preparation route dependence of conductivity was observed in the new composite system; however, the majority of the compositions prepared by route 1 exhibited a little higher σ values.

3. Conductivity enhancements of more than eight times from the annealed host and about three times from the quenched host were obtained for the composition $0.8(0.75\text{AgI}:0.25\text{AgCl}):0.2\text{SnO}_2$, which we refer to as the “optimum composition”.

In an earlier study [21], we reported that the conductivity of the optimum composition varies with the soaking time. We carried out a similar study on the samples of optimum composition, $0.8(0.75\text{AgI}:0.25\text{AgCl}):0.2\text{SnO}_2$, prepared at different soaking times, namely, 5 min, 10 min, 15 min, 30 min and 24 h. We observed, as before [21], that the sample with the 15 min soaking time attained the highest σ value. Lower and higher soaking times resulted in samples of decreased conductivity; the reason for this has already been discussed in our earlier paper [21].

Fig. 2 shows the temperature variation in the logarithm of the conductivity, σ , for different compositions of $(1-x)(0.75\text{AgI}:0.25\text{AgCl}):x\text{SnO}_2$, including the pure (annealed-and-quenched) host $(0.75\text{AgI}:0.25\text{AgCl})$. Table I lists the values of room-temperature conductivity, σ , pre-exponential factor, σ_0 , and activation energy, E_a , computed from the log σ versus $1/T$ Arrhenius plots in Fig. 2 in the temperature region 27–110 °C for different x . The

variation in E_a with x is shown as an inset in Fig. 2. As noted earlier in Fig. 1 and as is also obvious from Fig. 2 and Table I, the room-temperature conductivity increased up to $x = 0.2$ and then decreased for higher SnO_2 concentrations. The E_a versus x variation in the above temperature region followed the usual behaviour of most solid electrolyte systems, i.e., the increase or decrease in conductivity with increasing concentration of dispersoid particles is accompanied by a decrease or increase in activation energy. An activation energy minima ($E_a \approx 0.147$ eV) was obtained for the optimum composition $0.8(0.75\text{AgI}:0.25\text{AgCl}):0.2\text{SnO}_2$, indicating relatively easy ion transport at this composition. The enhancement in the room-temperature conductivity

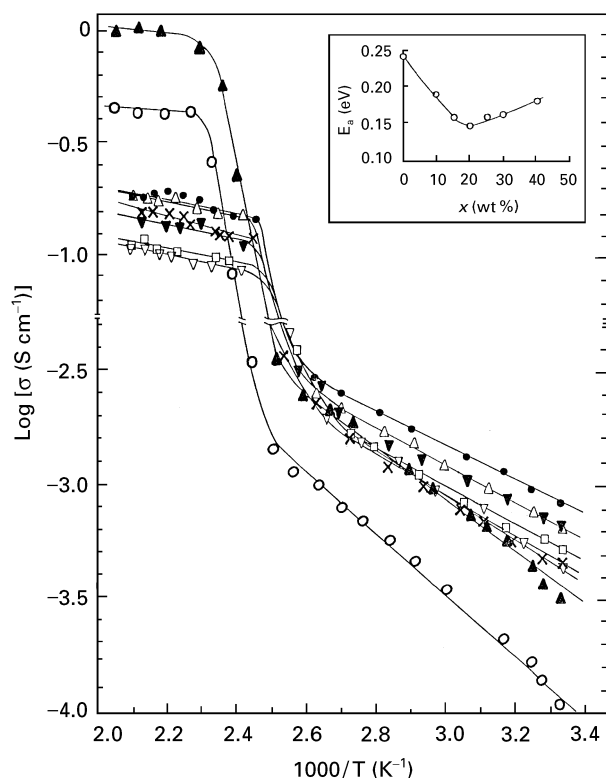


Figure 2 log σ versus $1/T$ plots for different compositions of the composite electrolyte system $(1-x)(0.75\text{AgI}:0.25\text{AgCl}):x\text{SnO}_2$ prepared by route 1. (○), pure annealed host; (▲), pure quenched host; (×), $x = 10$ wt %; (▼), $x = 15$ wt %; (●), $x = 20$ wt %; (△) $x = 25$ wt %; (□), $x = 30$ wt %; (▽), $x = 40$ wt %. The inset shows the variation in activation energy, E_a as a function of x in the temperature region 27–110 °C.

TABLE I Room-temperature conductivities, pre-exponential factors and activation energy values for various x of the composite system $(1-x)(0.75\text{AgI}:0.25\text{AgCl}):x\text{SnO}_2$ (temperature range, 27–110 °C)

x (wt %)	Conductivity $\sigma_{27^\circ\text{C}}$ (S cm^{-1})	Pre-exponential factor σ_0 (S cm^{-1})	Activation energy E_a (eV)
0	1.0×10^{-4} (pure annealed host)	1.78	0.243
0	3.1×10^{-4} (pure quenched host)	3.22	0.234
10	4.7×10^{-4}	0.66	0.190
15	6.9×10^{-4}	0.30	0.159
20	8.4×10^{-4}	0.25	0.147
25	6.7×10^{-4}	0.33	0.161
30	6.0×10^{-4}	0.28	0.163
40	4.7×10^{-4}	0.50	0.181

may be attributed to the increased mobile ion concentration in the host–dispersoid interface region and/or increased ionic mobility, as mentioned earlier in the introduction. Hence, for the present system, the reasons could be clearly understood on the basis of our mobility, μ , and mobile ion concentration, n , measurements, discussed below in Section 3.3.

3.2. Phase identification by X-ray diffraction and differential thermal analysis

The coexistence of separate phases is one of the essential requirements of two-phase composite systems. This indicates that the dispersion of second-phase particles has not introduced any chemical and/or structural changes into either of the phases. XRD and DTA techniques were used by us to identify the existence of two separate phases of the composite system: $0.8(0.75\text{AgI}:0.25\text{AgCl}):0.2\text{SnO}_2$.

Figs 3a, b, c and d show the XRD patterns for the optimum composition prepared with an annealed host, the optimum composition prepared with a quenched host, a pure annealed host and a pure quenched host, respectively. The full circles in Figs 3a and b correspond to SnO_2 reflections. On comparing the reflection peaks, it can very well be inferred that firstly no structural and chemical changes occurred in the host compound by the dispersion of SnO_2 particles and the two phases coexist separately in the composite system, and secondly almost identical reflection peaks occurred in the patterns in both Fig. 3a and Fig. 3b. This is indicative of the fact that the composite system prepared using an annealed and/or quenched host resulted in a similar optimum composition.

The above results were further supported by our DTA studies. Figs 4a and b show DTA curves for the pure quenched host and the optimum conducting composition, respectively. We note that the endothermic peak at about 135 °C, which corresponds to a characteristic $\beta \rightarrow \alpha$ -like transition temperature of the quenched host [18], remained unaffected in the composite system. This is again indicative of the fact that no chemical reaction and/or compound formation occurred during the sample preparation and the host exists as a separate phase in the system. In the interpretation of our XRD and DTA results, we compared the plots of the composite system with that of

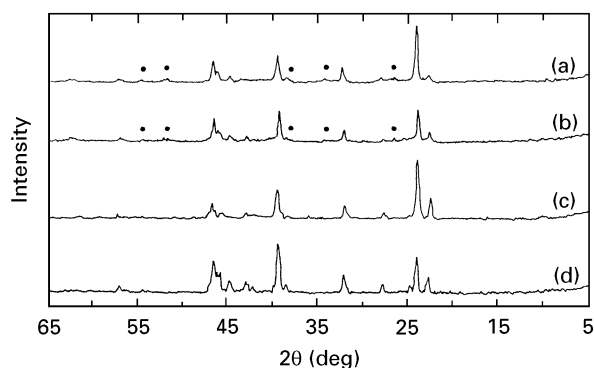


Figure 3 XRD patterns: (a) optimum composition 0.8(0.75AgI:0.25AgCl):0.2SnO₂ prepared with the annealed host; (b) optimum composition prepared with the quenched host; (c) pure annealed host; (d) pure quenched host. (●), SnO₂ peaks.

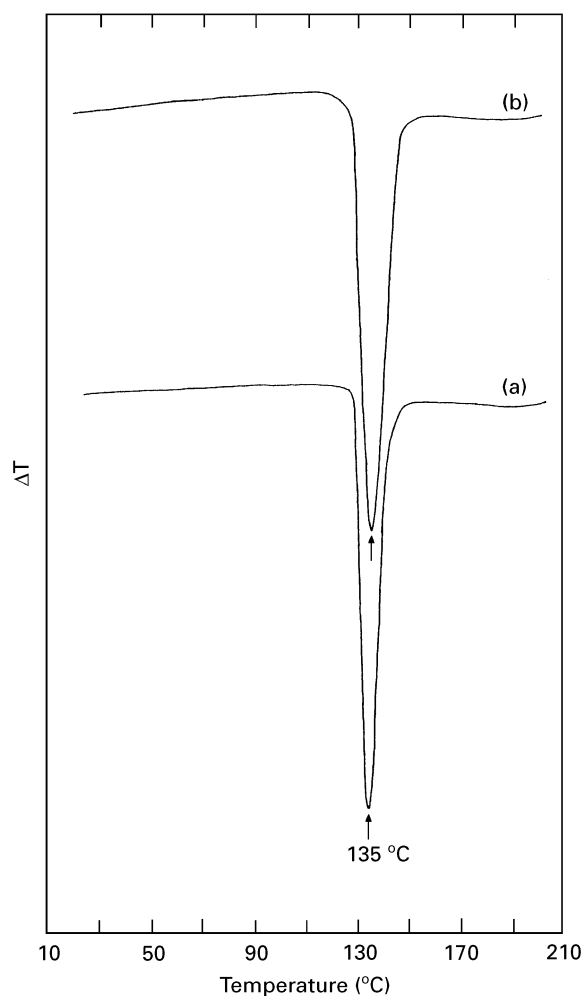


Figure 4 DTA curves: (a) pure quenched host (0.75AgI:0.25AgCl); (b) optimum composition 0.8(0.75AgI:0.25AgCl):0.2SnO₂.

the quenched host. This is because the composite systems prepared by route 1 (see Section 2) would contain a quenched host because of rapid cooling of the host–dispersoid mixture.

3.3. Ionic mobility and mobile ion concentration measurements

The conductivity of a solid ion-conducting composite electrolyte system is related to the mobile ion

concentration, n , and ionic mobility, μ , in the following way:

$$\sigma = nq\mu \quad (1)$$

where q is the charge on the mobile ion. When σ , μ and n are temperature dependent, the variation in these ionic parameters with temperature are governed by the following Arrhenius-type equations [21, 22, 25]:

$$\sigma = \sigma_0 \exp\left(-\frac{E_a}{kT}\right) \quad (2)$$

$$\mu = \mu_0 \exp\left(\mp\frac{E_m}{kT}\right) \quad (3)$$

$$n = n_0 \exp\left(\mp\frac{E_f}{kT}\right) \quad (4)$$

where σ_0 , μ_0 and n_0 are pre-exponential factors and E_a , E_m and E_f are the conductivity activation energy, the energy of migration and the energy of formation, respectively, which are related to each other as follows:

$$E_a = \pm E_m \pm E_f \quad (5)$$

The positive and negative signs in the argument of the above exponentials indicate the decrease and increase, respectively, in the factors on the left-hand side of the equations with increasing temperature. It is obvious from Equation 1 that the increase in σ involves an increase in either n or μ or both. For the two-phase composite system the reasons for conductivity enhancement in the first-phase host matrix could be assigned appropriately if μ and n values of both composite and host systems could be measured independently.

The direct determination of the Ag⁺ ion mobility, μ , in the composite system 0.8(0.75AgI:0.25AgCl):0.2SnO₂ was done by the transient ionic current technique [25–27]. The details of the experimental procedure have already appeared elsewhere in our recent papers [18–25]. However, the ionic mobility at any fixed temperature can be calculated using the following formula:

$$\mu = \frac{d^2}{V\tau} \quad (\text{cm}^2 \text{V}^{-1} \text{s}^{-1}) \quad (6)$$

where τ is the time taken by the Ag⁺ ion to cross the thickness d of the sample pellet after the polarity of the direct-current (d.c.) potential, V , applied across the pellet sandwiched between two blocking (graphite) electrodes, has been reversed.

The mobile Ag⁺ ion concentration, n , was calculated with the help of σ and μ values using Equation (1). Table II lists the room-temperature values of σ , μ and n for the optimum conducting composition 0.8(0.75AgI:0.25AgCl):0.2SnO₂ together with the values for pure annealed and pure quenched hosts. It can obviously be noted from Table II that the n value for the composite system is extremely close to the values for both pure annealed and pure quenched hosts obtained earlier by us [18]. However, an increase of approximately one order of magnitude in

TABLE II Room-temperature conductivities, ionic mobilities and mobile ion concentrations of pure (annealed-and-quenched) hosts and optimum composition

Material	Conductivity $\sigma_{27^\circ\text{C}}$ (S cm^{-1})	Mobility $\mu_{27^\circ\text{C}}$ ($\text{cm}^2 \text{V}^{-1} \text{s}^{-1}$)	Mobile ion concentration $n_{27^\circ\text{C}}$ (cm^{-3})
Host compound			
(0.75AgI:0.25AgCl) (annealed)	1.0×10^{-4}	$(1.5 \pm 1) \times 10^{-2}$	4.0×10^{16}
(0.75AgI:0.25AgCl) (quenched)	3.1×10^{-4}	$(2.4 \pm 1) \times 10^{-2}$	8.0×10^{16}
Composite system:			
0.8(0.75AgI:0.25AgCl):0.2SnO ₂	8.4×10^{-4}	$(1.4 \pm 1) \times 10^{-1}$	3.7×10^{16}

μ was obtained for the composite system compared with the μ values of pure hosts.

Hence, on the basis of these studies it can be safely concluded that the increase in ionic mobility is responsible for the conductivity enhancement in the present composite system 0.8(0.75AgI:0.25AgCl):0.2SnO₂. However, as mentioned earlier, the mobility increase in the two-phase composite system is directly associated with the creation of highly conducting intergrain paths. It has been reported in the literature [28] that SnO₂ introduces porosity in sintered ZnO pellets. A similar phenomenon is presumably occurring in our system during sample preparation. The creation of porosity increases the intergrain connectivity, which in turn results in enhanced ionic mobility. In a recent study by Shaju and Chandra [17] on a SnO₂-dispersed, highly conducting glass matrix (AgI + Ag₂O + B₂O₃) system, where the SnO₂ remained as a separate phase, the enhancement in the room-temperature conductivity reported was also due to the enhancement in the Ag⁺ ion mobility in the space-charge region. They proposed a space-charge model for this enhanced mobility involving the concept of a mobile ion concentration gradient near or at the interface in the space-charge region [17]. According to their hypothesis, the migrating ions emanating from the host salt and falling inside or near the space-charge region find a relatively free migration pathway. Hence, near the surface of the host salt inside the space-charge region, the mobile ions can move with relative ease, involving a relatively lower migration energy.

The μ and n measurements were also carried out on the optimum composition 0.8(0.75AgI:0.25AgCl):0.2SnO₂ at different temperatures. Fig. 5 shows the $\log \mu$ versus $1/T$ and $\log n$ versus $1/T$ plots together with the $\log \sigma$ versus $1/T$ plot of Fig. 2 for the optimum composition which is redrawn to enable direct comparison. These variations follow the thermally activated type of behaviour in both temperature regions (regions I and II) and can be expressed by the Arrhenius-type Equations (2–4). Some interesting observations of this study can be noted as follows.

1. σ increased steadily with increasing temperature in region I, followed by an abrupt jump (about 10^2) at approximately 135 °C (i.e., the $\beta \rightarrow \alpha$ transition temperature of the host [18]) and then remained almost constant in region II.

2. μ and n also increased with increasing temperature in region I, similar to σ , but with a relatively

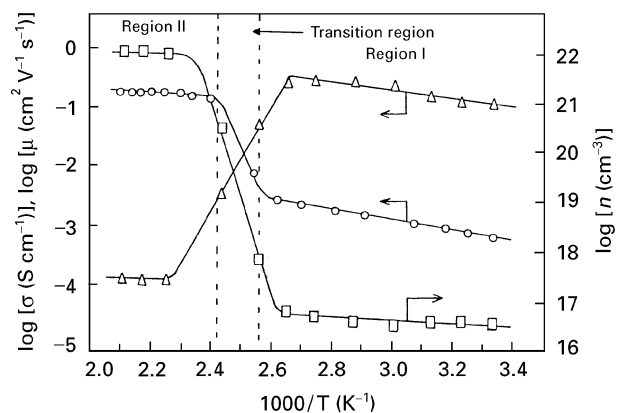


Figure 5 $\log \mu$ versus $1/T$ (Δ) and $\log n$ versus $1/T$ (\square) Arrhenius plots for the optimum composition 0.8(0.75AgI:0.25AgCl):0.2SnO₂. The $\log \sigma$ versus $1/T$ (\circ) plot of Fig. 2 for this composition is redrawn.

slower rate. The abrupt decrease in μ and increase in n occurs at about 100 °C, and then both become almost independent of temperature in region II.

We obtained almost similar variations in σ , μ and n with increasing temperature earlier for the host and Al₂O₃-dispersed composite system [18, 21]. The onsets of the abrupt changes in μ and n in the present system well below the transition temperature (about 135 °C) are attributed to pre-transition effects, as before. Following the line of arguments given in our recent papers [18, 21], the decrease in μ (in region II) is due to the structural space narrowing of the α -like phase of the host as well as to the blocking effect of dispersoid particles. The abrupt increase in n (in region II) is due to the availability of a large number of equi-energetic mobile Ag⁺ ions in the α -like phase of the host. Table III lists the values of the pre-exponential factors, σ_0 , μ_0 and n_0 , and energies, E_a , E_m and E_r computed from the Arrhenius plots in Fig. 5. It can be obviously seen from Table III that the values of E_a , E_m and E_r satisfy Equation (5) very well in both the temperature regions (regions I and II).

3.4. Temperature dependence of the ionic transference number, t_{ion} , and drift velocity, v_d

The above experimental measurements on μ and n are well supported by the temperature dependence studies of the ionic transference number, t_{ion} , using Wagner's

TABLE III Pre-exponential factors, σ_0 , μ_0 and n_0 and energies, E_a , E_m and E_f , calculated from the plots in Fig. 5

Temperature region	$\sigma = \sigma_0 \exp(-E_a/kT)$		$\mu = \mu_0 \exp(\mp E_m/kT)$		$n = n_0 \exp(\mp E_f/kT)$	
	σ_0	E_a (eV)	μ_0	E_m (eV)	n_0	E_f (eV)
I	0.25	0.147	$1.1 \times 10^{+1}$	0.111	1.5×10^{17}	0.036
II	0.67	0.052	1.7×10^{-4}	0.010	2.5×10^{22}	0.042

d.c. polarization method. The transference number is the quantitative measure of the ionic and electronic contributions to the total conductivity of the system. For experimental details, reference may be made to our recent papers [18, 21, 22]. A d.c. potential (about 0.5 V) is applied across the sample pellet sandwiched between blocking (graphite) and non-blocking (silver metal) electrodes and the current (in arbitrary units) is monitored as a function of time. Fig. 6 shows the current versus time plots for the sample pellets of optimum composition kept at various temperatures, namely 27, 47, 67, 87 and 107 °C (region I) and 167, 187 and 207 °C (region II). Some of the significant observations of this study are the following.

1. The values of total current decreased to zero at all temperatures. This is indicative of the fact that the system remained purely ionic (i.e., $t_{ion} \approx 1$) throughout the temperature range of operation, as also shown in the inset of Fig. 6.

2. The value of the initial current, I_T , as marked in Fig. 6 increased with increase in temperature, which in turn indicated an increase in n . This supports well our earlier results on $\log n$ versus $1/T$ variation.

3. The polarizing time (i.e., the time for which the total current approached zero) increased with increasing sample temperature. This looks logical. At higher temperatures the mobile ions are relatively more thermally agitated than at lower temperatures; hence, longer time durations would be required for them to become polarized at a constant fixed potential.

Using the value of the initial current, I_T , the ionic drift velocity, v_d (in arbitrary units), as a function of temperature, was evaluated with the help of the following equation [22]:

$$v_d = \frac{I_T}{Anq}$$

where A is the area of the sample pellet, q is the charge on a mobile ion and n is the number of charge carriers obtained from the $\log n$ versus $1/T$ variation in Fig. 5. Fig. 7 shows the $\log v_d$ versus $1/T$ plot for the optimum composition 0.8(0.75AgI:0.25AgCl):0.2SnO₂. The Arrhenius equations, governing this variation in the two temperature regions, can be expressed as

$$v_d = 1.8 \times 10^{-1} \exp\left(-\frac{0.126}{kT}\right) \quad \text{region I}$$

$$v_d = 7.1 \times 10^{-7} \exp\left(-\frac{0.008}{kT}\right) \quad \text{region II}$$

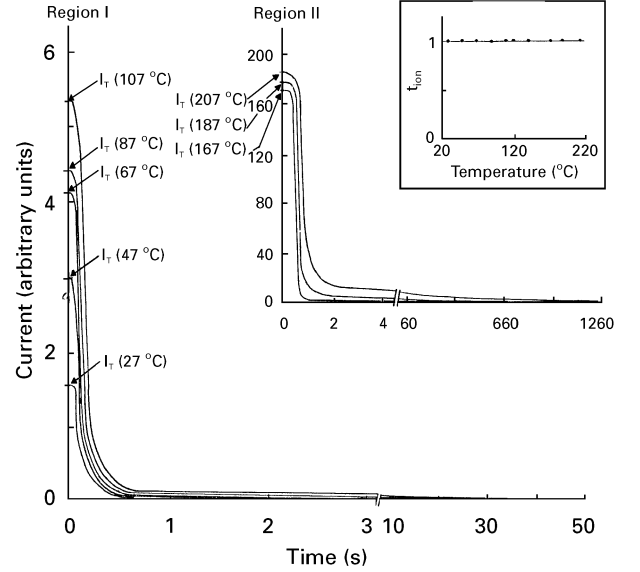


Figure 6 Current versus time plots at various temperatures (given in parentheses) for the measurement of the ionic transference number, t_{ion} , on the optimum composition 0.8(0.75AgI:0.25AgCl):0.2SnO₂. The inset shows t_{ion} as a function of temperature.

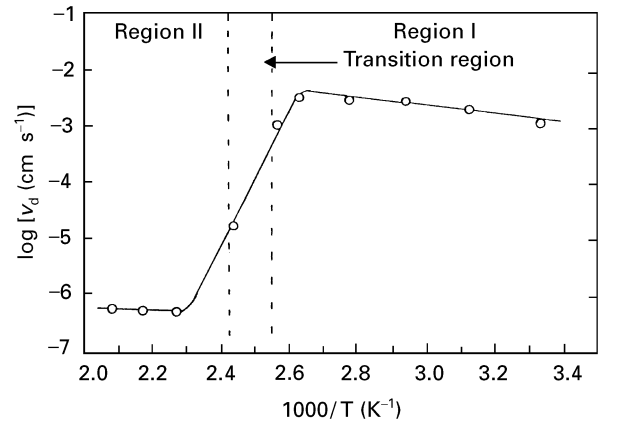


Figure 7 $\log v_d$ versus $1/T$ Arrhenius plot for the optimum composition: 0.8(0.75AgI:0.25AgCl):0.2SnO₂.

where 0.126 eV and 0.008 eV are the energies, E_d , involved in the above thermally activated process. Since, at a fixed value of d.c. polarizing potential (i.e., about 0.5 V in the present case), the ionic drift velocity is directly proportional to the ionic mobility at all temperatures. Hence, the $\log v_d$ versus $1/T$ variation should be identical to the $\log \mu$ versus $1/T$ variation. One can obviously note from Figs 5 and 7 that these variations are almost identical. Also, the E_d values

of 0.126 eV (region I) and 0.008 eV (region II) obtained above are reasonably close to the E_m values of 0.111 eV (region I) and 0.01 eV (region II), respectively, obtained earlier. The small deviation is due to our experimental limitations in measuring the initial current, I_T , accurately at $t \approx 0$ s.

4. Conclusions

Conductivity enhancements in a two-phase composite electrolyte system 0.8(0.75AgI:0.25AgCl):0.2SnO₂ are reported at room temperature. The conventional first-phase host matrix AgI has been replaced by an alternative compound “a quenched-and-annealed (0.75AgI:0.25AgCl) mixed system”. On the basis of various experimental studies performed on the present composite system, the following conclusions can be drawn.

1. The conductivity enhancement at room temperature is predominantly due to the increased ionic mobility as a result of ‘porosity’ introduced in the system by second-phase dispersoid SnO₂ during sample preparation, which in turn increased the inter-grain connectivity.

2. The increase in conductivity, σ , with increasing temperature in region I is due to the increase in the mobility, μ , as well as in the mobile ion concentration, n . Whereas σ , μ and n remained almost constant in region II. The large increase in n after the transition region not only compensated the sharp decrease in μ well but also gave rise to a net increase in σ during the transition from region I to region II.

3. The system remained purely ionic as revealed by the temperature dependence of the ionic transference number. The ionic drift velocities at different temperatures were determined from these measurements. This study supported our above results on μ and n measurements well.

Acknowledgements

We are grateful to professor S. Chandra for providing DTA and XRD facilities. We also thank Dr A. Chandra and Mr K. M. Shaju, Physics Department, Banaras Hindu University, Varanasi, for their help during the structural and thermal characterization studies. We are grateful to the University Grants Commission for the financial assistance extended to us through Project F-10-4/90 (SR-I) dt. 11/07/91.

References

1. K. SHAHI and J. B. WAGNER, Jr, *J. Solid State Chem.* **42** (1982) 107.
2. J. MAIER, in “Superionic solids and solid electrolytes – recent trends”, edited by A. L. Laskar and S. Chandra (Academic Press, New York, 1989) p. 137.
3. N. J. DUDNEY, *Ann. Rev. Mater. Sci.* **19** (1989) 103.
4. J. B. WAGNER, Jr., in “High conductivity solid ionic conductors—recent trends and applications”, edited by T. Takahashi (World Scientific, Singapore, 1989) p. 146.
5. M. C. R. SHASTRY and K. J. RAO, *Solid State Ionics* **51** (1992) 311.
6. A. K. SHUKLA and V. SHARMA, in “Solid state ionics—materials and applications”, edited by B. V. R. Chowdari, S. Chandra, S. Singh and P. C. Srivastava (World Scientific, Singapore, 1992) p. 91.
7. T. TAKAHASHI, in “Solid state ionic materials”, edited by B. V. R. Chowdari, M. Yahaya, I. A. Talib and M. M. Salleh (World Scientific, Singapore, 1994) p. 15.
8. T. JOW and J. B. WAGNER, Jr., *J. Electrochem. Soc.* **126** (1979) 1963.
9. J. MAIER, *Phys. Status Solidi (b)* **123** (1984) K89.
10. *Idem.*, *ibid.* **124** (1984) K187.
11. *Idem.*, *J. Phys. Chem. Solids* **46** (1985) 309.
12. *Idem.*, *Mater. Res. Bull.* **20** (1985) 383.
13. A. BUNDE, W. DIETERICH and E. ROMAN, *Phys. Rev. Lett.* **55** (1985) 5.
14. R. BLENDER and W. DIETERICH, *J. Phys. C* **20** (1987) 6113.
15. N. F. UVAROV, V. P. ISUPOV, V. SHARMA and A. K. SHUKLA, *Solid State Ionics* **51** (1992) 41.
16. U. LAUER and J. MAIER, *ibid.* **51** (1992) 209.
17. K. M. SHAJU and S. CHANDRA, *J. Mater. Sci.* **30** (1995) 3457.
18. R. C. AGRAWAL, R. K. GUPTA, R. KUMAR and A. KUMAR, *J. Mater. Sci.* **29** (1994) 3673.
19. R. C. AGRAWAL, R. KUMAR, R. K. GUPTA and M. SALEEM, *J. Non-Cryst. Solids* **181** (1995) 110.
20. R. K. GUPTA and R. C. AGRAWAL, *Solid State Ionics* **72** (1994) 314.
21. R. C. AGRAWAL and R. K. GUPTA, *J. Mater. Sci.* **30** (1995) 3612.
22. R. C. AGRAWAL and R. KUMAR, *J. Phys. D* **27** (1994) 2431.
23. *Idem.*, in “Solid state ionic materials”, edited by B. V. R. Chowdari, M. Yahaya, I. A. Talib and M. M. Salleh (World Scientific, Singapore, 1994) p. 295.
24. *Idem.*, *J. Phys. D* **29** (1996) 156.
25. R. C. AGRAWAL, K. KATHAL and R. K. GUPTA, *Solid State Ionics* **74** (1994) 137.
26. M. WATANABE, K. SANUI, N. OGATA, T. KOBAYASHI and Z. ONTAKI, *J. Appl. Phys.* **57** (1985) 123.
27. S. CHANDRA, S. K. TOLPADI and S. A. HASHMI, *Solid State Ionics* **28–30** (1988) 651.
28. T. KIMURA, S. INADA and T. YAMAGUCHI, *J. Mater. Sci.* **24** (1989) 220.

Received 22 June 1995

and accepted 19 December 1996